Lightning in Wildfire Smoke Plumes Observed in Colorado during Summer 2012

TIMOTHY J. LANG

NASA Marshall Space Flight Center, Huntsville, Alabama

STEVEN A. RUTLEDGE AND BRENDA DOLAN

Colorado State University, Fort Collins, Colorado

PAUL KREHBIEL AND WILLIAM RISON

New Mexico Institute of Mining and Technology, Socorro, New Mexico

DANIEL T. LINDSEY

NOAA/NESDIS/STAR/RAMMB, Fort Collins, Colorado

(Manuscript received 3 June 2013, in final form 28 August 2013)

ABSTRACT

Pyrocumulus clouds above three Colorado wildfires (Hewlett Gulch, High Park, and Waldo Canyon; all during the summer of 2012) electrified and produced localized intracloud discharges whenever the smoke plumes grew above 10 km MSL (approximately −45°C). Vertical development occurred during periods of rapid wildfire growth, as indicated by the shortwave infrared channel on a geostationary satellite, as well as by incident reports. The lightning discharges were detected by a three-dimensional lightning mapping network. Based on Doppler and polarimetric radar observations, they likely were caused by ice-based electrification processes that did not involve significant amounts of high-density graupel. Plumes that did not feature significant amounts of radar-inferred ice at high altitudes did not produce lightning, which means lightning observations may assist in diagnosing pyrocumulus features that could affect the radiative characteristics and chemical composition of the upper troposphere. The lightning was not detected by the National Lightning Detection Network, implying that pyrocumulus lightning may occur more frequently than past studies (which lacked access to detailed intracloud information) might suggest. Given the known spatial and temporal advantages provided by lightning networks over radar and satellite data, the results also indicate a possible new application for lightning data in monitoring wildfire state.

1. Introduction

Pyrocumulus clouds frequently occur over wildfires, often growing to high altitudes and impacting chemical composition and aerosol concentrations in the upper troposphere (Fromm et al. 2010). On occasion, these clouds also have been observed to electrify and produce lightning (Latham 1991; Rosenfeld et al. 2007). Interestingly, observed cloud-to-ground (CG) lightning flashes from these clouds, or other thunderstorms ingesting smoke, will often transfer a predominantly positive charge to the ground (Latham 1991; Lyons et al. 1998; Rosenfeld et al. 2007; Rudlosky and Fuelberg 2011). This phenomenon is not particularly well understood, but may depend on increased supercooled liquid water due to intensification of thunderstorm updrafts (Williams et al. 2005; Lang and Rutledge 2006; Rosenfeld et al. 2007) via aerosol-based suppression of warm-rain microphysical processes (Rosenfeld 1999; Andreae et al. 2004; Khain et al. 2008). On the other hand, it may occur because of a preferential increase in concentration of certain ions that exist within wildfire smoke (Vonnegut et al. 1995; Latham 1999; Jungwirth et al. 2005).

A notable deficiency in previous studies of pyrocumulus electrification is the lack of three-dimensional lightning mapping data, such as those provided by the Lightning Mapping Array (LMA) system developed by the New Mexico Institute of Mining and Technology

Corresponding author address: Timothy J. Lang, NASA Marshall Space Flight Center (ZP11), Huntsville, AL 35812.
E-mail: timothy.j.lang@nasa.gov

DOI: 10.1175/MWR-D-13-00184.1

(Rison et al. 1999). These systems have been useful for identifying and understanding electrification under exotic meteorological scenarios, such as volcanic plumes (Thomas et al. 2007; Behnke et al. 2012) and lightning initiation within thunderstorm anvils (Kuhlman et al. 2009). Although Doppler radar has been exploited in the study of wildfire smoke plumes and pyrocumulus (Hufford et al. 1998; Rosenfeld et al. 2007), polarimetric radar has not, despite its notable ability to identify smoke particles and distinguish them from precipitation (Melnikov et al. 2008, 2009; Jones et al. 2009). The use of multiple-Doppler wind retrievals in plumes is also very rare.

In this study, polarimetric and multiple-Doppler radar data are combined with LMA data to examined pyrocumulus electrification, based on observations from the Deep Convective Clouds and Chemistry (DC3) field campaign. DC3 took place during May–June 2012 in Colorado, Oklahoma, Texas, and Alabama, and was primarily focused on the chemical impacts of thunderstorms on the upper troposphere (Barth et al. 2013). However, radar and lightning ground facilities in Colorado also observed three distinct instances (on 16 May 2012, as well as on 13 and 26 June) of pyrocumulus electrification and lightning production over three separate wildfires (Hewlett Gulch, High Park, and Waldo Canyon). The unique dataset revealed electrification behavior—including the production of localized intracloud (IC) flashes—that may depend crucially on fire and smoke plume evolution. This suggests potential new applications for lightning data in monitoring wildfires. One is identifying explosive wildfire growth that occurs under specific meteorological conditions. Another is indicating the presence (or lack thereof) of significant amounts of precipitation-sized ice at high altitudes, which has implications for the radiative characteristics and chemical composition of the upper troposphere. The data also suggest that pyrocumulus electrification—particularly that which produces only IC lightning—occurs more often than what conventional very low-frequency/low-frequency (VLF/LF) lightning networks, such as the National Lightning Detection Network (NLDN; which did not detect the pyrocumulus lightning over these fires), would indicate.

2. Data and methodology

a. Radar

The Colorado State University–University of Chicago–Illinois State Water Survey (CSU–CHILL) radar is an S-band polarimetric Doppler radar with a unique dual-offset Gregorian antenna that provides high-quality polarization observations (Bringi et al. 2011). The radar was operated during DC3 in an alternate transmit and receive mode, which provides linear depolarization ratio (LDR) in addition to other standard polarimetric variables, and avoids cross-coupling issues in differential reflectivity Z_{DR}. DC3 scanning strategies commonly involved coordinated plan position indicator (PPI) dual-Doppler sector volumes with the CSU–Pawnee radar, along with interspersed scan volumes in range–height indicator (RHI) format.

The CSU–Pawnee radar is an S-band Doppler radar used for dual-Doppler PPI sector scanning with the CSU–CHILL radar (along a baseline of roughly 40 km; Lang and Rutledge 2002). During the Hewlett Gulch case, PPI-based dual-Doppler volumes were synchronized every 5 min, except for the 1945–1950 UTC volume when CSU–CHILL did RHI scans through the Hewlett Gulch plume at the same time it first produced lightning.

Data from CSU–CHILL and CSU–Pawnee radars, as well as the National Oceanic and Atmospheric Administration's (NOAA's) Cheyenne (KCYS) and Denver (KFTG) S-band Doppler radars, were subjected to appropriate quality control. Then they were synthesized to derive three-dimensional wind fields using the National Center for Atmospheric Research's (NCAR's) Custom Editing and Display of Reduced Information in Cartesian Space (CEDRIC) software (Mohr et al. 1986). The anelastic mass-continuity assumption used in the derivation of the vertical wind may not be completely valid given the continuous heat source of the fire. As such, this technique likely provides a lower bound on the vertical wind. Each radar was gridded to a common Cartesian grid centered on CSU–CHILL with 1-km resolution in x, y, and z using the NCAR Sorted Position Radar Interpolator (SPRINT) software (Mohr and Vaughn 1979; Miller et al. 1986), except in the case of CSU–CHILL RHI volumes, which were gridded with the NCAR Reorder software package (https://wiki.ucar.edu/display/raygridding/Reorder+Gridding+Software). More detailed information about the gridding and multiple-Doppler synthesis methodology is outlined in Dolan and Rutledge (2007).

The NOAA National Mosaic and MultiSensor Quantitative Precipitation Estimation (NMQ) system provides three-dimensional radar mosaics covering the entire contiguous United States (Zhang et al. 2011). These mosaics originate from the nationwide network of S-band Doppler weather radars, which in the Colorado DC3 domain means the most important contributors are the Denver (KFTG), Cheyenne (KCYS), and Pueblo (KPUX) radars. These radars were not yet upgraded to be polarimetric by the time of DC3. Mosaic radar reflectivity is available every 5 min on a 0.01° latitude–longitude grid, with a vertical coordinate that ranges from 0.25 km MSL to 18 km (vertical spacing is 0.25 km near the surface gradually stretching to 2 km aloft).

b. Lightning

The Colorado Lightning Mapping Array (COLMA) was installed by the New Mexico Institute of Mining and Technology prior to the start of the DC3 field campaign (Krehbiel et al. 2012). The system consisted of 15 sensors distributed throughout northeastern Colorado and provided continuous lightning observations throughout the summer of 2012. Full-rate (i.e., not decimated) data were used in the analysis. A minimum of seven station detections and a chi-squared error of 1 or less were required for a location solution, similar to past LMA studies (e.g., Lang and Rutledge 2011). COLMA coverage over the region burned by the Hewlett Gulch (~80 km from network center) and High Park fires (~85-km range) was excellent, with altitude location errors expected to be ~100 m or less, based on a pre-DC3 modeling study. Coverage over the Waldo Canyon fire (near Colorado Springs; ~200-km range) was poorer, with vertical errors expected to be greater than 300 m. Based on the DC3 experience, the performance characteristics and location accuracy of this network appears better than most, if not all, previously deployed LMA networks (e.g., Thomas et al. 2004; Goodman et al. 2005; MacGorman et al. 2008). Flash rates were calculated via the same methodology as Lang and Rutledge (2008), which used fairly standard space–time criteria to separate flashes. A map of the Colorado DC3 domain, showing the locations of COLMA stations and the CSU radars, is shown in Fig. 1.

Flash-level data from the NLDN were also examined in the vicinity of the three wildfires. The NLDN, a nationwide network of VLF/LF sensors, detects and locates in two dimensions (latitude–longitude) ~95% of CGs and 25%–30% of ICs, with spatial errors <0.5 km (Cummins and Murphy 2009). During their respective analysis periods (encompassing each plume lightning episode), no NLDN-detected lightning of any type (IC or CG) occurred near either the fires or smoke plumes, nor were any NLDN-detected flashes associated with any of the LMA-mapped lightning presented in this study.

c. Satellite

Geostationary Operational Environmental Satellite (GOES) data were obtained from the Cooperative Institute for Research of the Atmosphere (CIRA) archive. *GOES-13*, which is centered at 75°W longitude, was used for 2 days of this study (16 May and 13 June 2012). *GOES-15* (centered at 135°W) was used for 26 June. Infrared (IR) bands 2 (centered at 3.9 μm) and 4 (centered at 10.7 μm), both with a subpoint resolution of 4 km, were examined for the three Colorado fire cases. Infrared pixel sizes over Colorado are approximately 4 km × 7 km. The 3.9-μm band is sensitive to subpixel heat sources (Weaver et al. 2004), and thus is useful for locating the hot spots associated with fires. Band 4 is the window IR band and is used to estimate cloud-top temperatures. During 13 June (High Park fire), *GOES-13* was in normal operational mode, providing 15-min updates except during the 3-hourly full-disk scans, when the spacing became 30 min. *GOES-13* was in rapid scan operation (RSO) on 16 May (Hewlett Gulch fire), which meant the continental United States was scanned more often than during regular operations. *GOES-15* was in RSO on 26 June (Waldo Canyon fire). The RSO scanning schedule is irregular, but there are scans as frequent as every 5 min, and as infrequent as every 30 min (during the 3-hourly full-disk scans).

d. Soundings

Sounding information was taken from the local Denver, Colorado, sounding on each day. The morning (1200 UTC) and afternoon (0000 UTC) soundings from each day showed deep dry adiabatic layers from the surface (or above a surface-based inversion) up to 580–400 hPa (from −5° to −25°C), the range of altitudes on the different days in which the lifting condensation level (LCL) resided. Notably, this means there was not a warm cloud layer during these days, which is typical for drought periods in Colorado (Lang and Rutledge 2006). Above the LCL, lapse rates decreased somewhat but generally followed a moist-adiabatic profile. These profiles were supportive of the high-based convection that frequently produced gust fronts, as well as the deep vertical development of the smoke plumes that were observed on the lightning days.

3. Results

a. Hewlett Gulch fire

The Hewlett Gulch fire was an accidental human-caused fire that began on 14 May 2012 and was 100% contained by 22 May. In the interim, it burned 7685 acres (3110 ha) in a forested region northwest of Fort Collins, Colorado (Inciweb 2013a). The only known instance of lightning-producing pyroconvection for this fire occurred on the afternoon of 16 May, when elevated convective activity with gusty downdrafts occurred over the foothills. This stirred up the fire, which spread by more than 4000 acres (1619 ha) on this particular day. Pyrocumulus were observed to form atop the smoke plume during the early afternoon. Merging the 1200 UTC (15 May) and 0000 UTC (16 May) soundings placed the LCL near 560–580 hPa (about −5° to −10°C, or 4.5–4.9 km MSL). The freezing altitude was 4.1–4.3 km MSL, and the −40°C

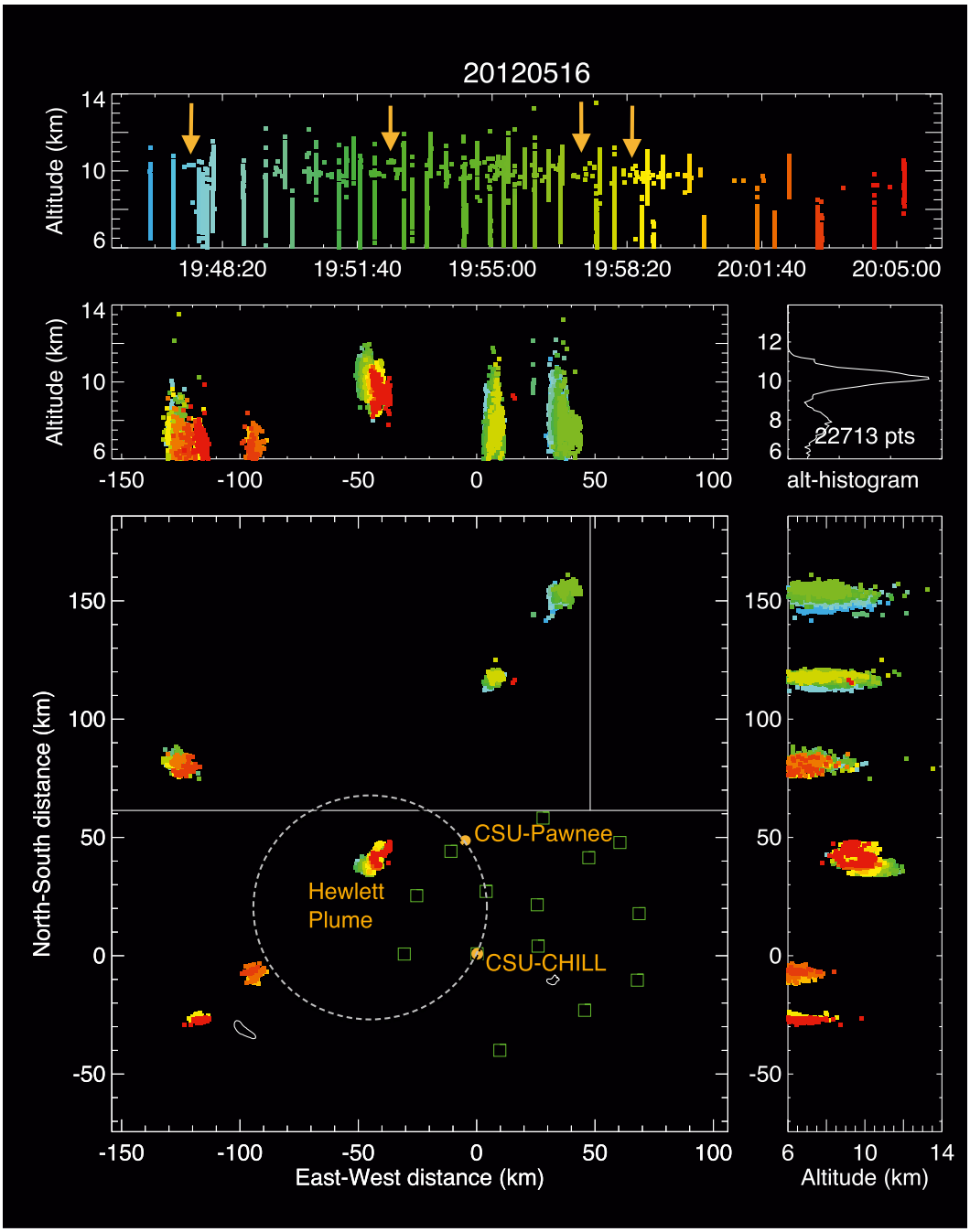

FIG. 1. Large-scale view of COLMA-detected VHF sources during the period of Hewlett Gulch plume lightning (1948–2005 UTC 16 May 2012). (top) Time–height plot, COLMA sources are colored by the times indicated. (middle left) *X*–*Z* projection, (middle right) source altitude histogram, (bottom left) plan (*X*–*Y*) view, and (bottom right) *Y*–*Z* projection. Distances are relative to CSU–CHILL, and altitudes are km MSL. Also shown in the plan view are COLMA station locations (open green squares), state boundaries (solid white lines), radar locations (orange dots), and the western dual-Doppler lobe for the CSU–CHILL/Pawnee pair (gray dashed circle). Select examples of plume lightning precursor sources are indicated by the orange arrows in (top).

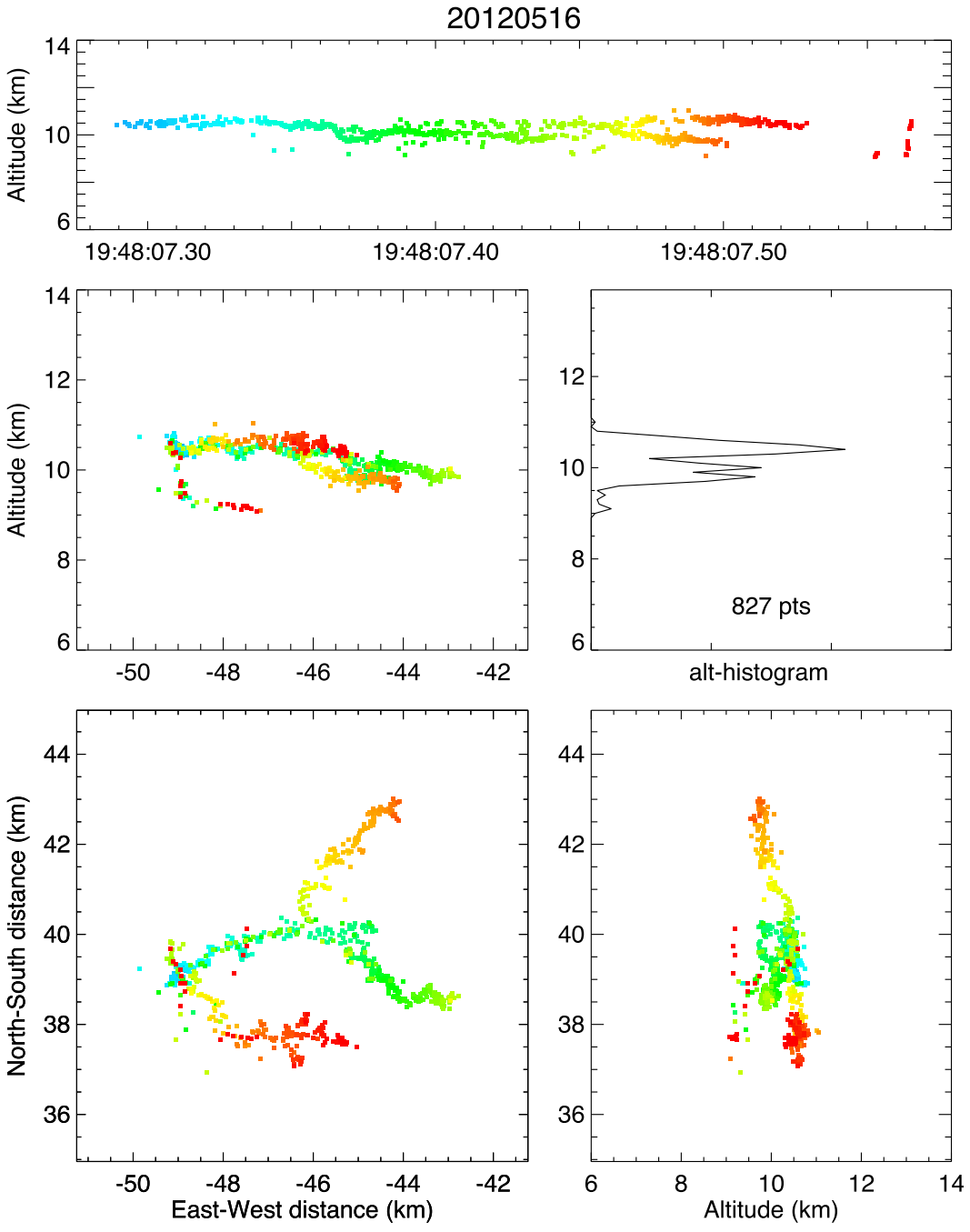

FIG. 2. As in Fig. 1, but for COLMA map of the first flash in the Hewlett Gulch pyrocumulus on 16 May 2012 with sources colored by UTC time [as indicated in (top)].

level was 9.1–9.2 km MSL. Winds above 9 km MSL were primarily from the west–southwest (WSW) with speeds $\sim$10 m s^{-1}. As will be seen, this flow regime had important effects on the structure of the plume and the placement of the lightning within it.

The CSU–CHILL and Pawnee radars performed coordinated scanning over the Hewlett Gulch fire area starting at 1905 UTC. The primary target of the scanning was the smoke plume, which was readily apparent in the data from both radars, because of its relative isolation and unique characteristics (explained below). After 2220 UTC the radars changed targets to other convection in the area.

The first flash atop the Hewlett Gulch plume occurred at 1948 UTC (Fig. 2), and was noticed immediately by

CSU–CHILL radar scientists due to the real-time COLMA data feed available at the radar facility. CSU–CHILL and Pawnee had been scanning the plume the whole time, thereby providing radar coverage of the plume as it evolved and electrified. The plume was well centered within the western CSU–CHILL/Pawnee dual-Doppler lobe, at a range of 60–65 km from CSU–CHILL (Fig. 1).

The flash in Fig. 2 was a spatially compact IC flash, typical of the 20 flashes (consisting of >10 LMA sources) produced within the plume from 1948 to 2005 UTC (Fig. 1), for an average flash rate of 1.2 min^{-1}. It initiated just below 10 km MSL (which was approximately −46°C), and based on the initial upward motion of negative leaders appeared to discharge positive charge immediately above this altitude, and negative charge below, thus identifying it as a normal-polarity IC (Rison et al. 1999). However, the vertical span of the discharge did not significantly exceed 2 km. In addition, the flash did not significantly exceed 5 km in horizontal size in either direction.

LMA-mapped leaders within the flash propagated largely toward the north and east, which was consistent with charged particles advecting with the sounding-measured winds at this altitude. This flash, and most of the others occurring within the plume, were preceded by approximately 30 s of precursor activity (examples of precursors are shown in Figs. 1 and 3), which manifested itself as single LMA sources occurring every 3–5 s, very near (<1–2 km horizontal distance) the eventual initiation location for each flash. These precursors, which behaved like the initial pulses of larger flashes, are inferred to be VHF radiation associated with breakdown that failed to evolve into complete flashes (Krehbiel et al. 2003). The high altitude of the plume lightning distinguished it from other, conventional lightning-producing convection in the region (Fig. 1). Via the methodology of Rison et al. (1999), charge layers were inferred for all the plume lightning flashes, with the integrated results shown in Fig. 3. A notable result of this analysis is the gradual descent of the positive dipole toward the northeast, consistent with the gravitational settling of charged particles outside the core of the plume. For visualization purposes, the precursors are identified as negative-charge sources in Fig. 3, and are most easily seen in the time–height plot, in between the distinct flashes (which appear as near-vertical lines of sources).

Vertical projections of the plume's evolution are shown in Fig. 4. The smoke portion of the plume was apparent in the polarimetric data because of low reflectivities (10–25 dBZ; Figs. 4a–c), elevated Z_{DR} values (1–5 dB; Figs. 4d–f), and very low correlation coefficients ($\rho_{HV} \sim 0.6$ or less; not shown). These observations were entirely consistent with past observations of smoke plumes—which tend to contain large, nonspherical ash particles that fall with their major axis oriented horizontally—by polarimetric weather radars (Melnikov et al. 2008, 2009; Jones et al. 2009). At 1915 UTC, the most reflective portions of the plume were confined below 10 km MSL, and updrafts were modest (Figs. 4a,d,g). However, by 1935 UTC, a broad updraft region with speeds in excess of 6 m s^{-1} developed within the plume (Fig. 4h), driving echo tops to about 12 km (Fig. 4b). Some, but not all, of this ''overshooting'' echo contained elevated Z_{DR} values characteristic of smoke and ash particles (>1 dB; Fig. 4e). By the last volume shown in Fig. 4, lightning was well under way and the echo tops remained above 10 km, although updraft strength had weakened considerably (now everywhere <3 m s^{-1}; Figs. 4c,f,i).

Lightning was favored in regions of decreased Z_{DR} (Fig. 4f), a result confirmed by more detailed investigation of the COLMA-detected lightning overlaid on polar-coordinate CSU–CHILL data (Fig. 5). In fact, between ranges 57 and 65 km from the radar and 9 and 11 km MSL (−40° to −55°C)—a region containing 99% of all VHF sources in this flash—mean Z was 18.2 dBZ and mean Z_{DR} was 0.3 dB, which is not consistent with the presence of high-density graupel (Vivekanandan et al. 1999, their Fig. 3). However, mean ρ_{HV} was only 0.64 in this region, indicating that a mixture of particles (likely ice and ash) was still present (ρ_{HV} in pure ice is typically >0.95; Tessendorf et al. 2005).

The gradual decrease in Z_{DR} and increase in ρ_{HV} with height in Fig. 5 (particularly above the LCL) suggest increasing contributions of frozen hydrometeors to the reflectivities higher up in the plume. Relatively clean (i.e., ash free), stratified ice cloud, indicated by low Z_{DR} (<1 dB) and increased ρ_{HV} (>0.8 in areas despite the low reflectivities of ~10 dBZ), existed on either side of the plume (which likely contained a mixture of ash and ice) near 6–8 km MSL. The pyroconvective plume had penetrated through this midlevel ''clean'' cloud layer. Significant amounts of high-density graupel, which would have been indicated by high reflectivities (>30 dBZ) along with Z_{DR} near 0 dB (e.g., Fig. 3 of Vivekanandan et al. 1999; Table 2 of Tessendorf et al. 2005), were not observed at any location in or near the pyroconvection during the analysis period.

Other polarimetric parameters were examined, though not shown here. LDR was generally large (>−15 dB) throughout the plume, consistent with the low reflectivities (and thus reduced signal-to-noise ratio for cross-polar returns, which increases LDR when $Z < 35$ dBZ) as well as the presence of irregularly shaped particles like ash. Differential phase was noisy, particularly within the lower

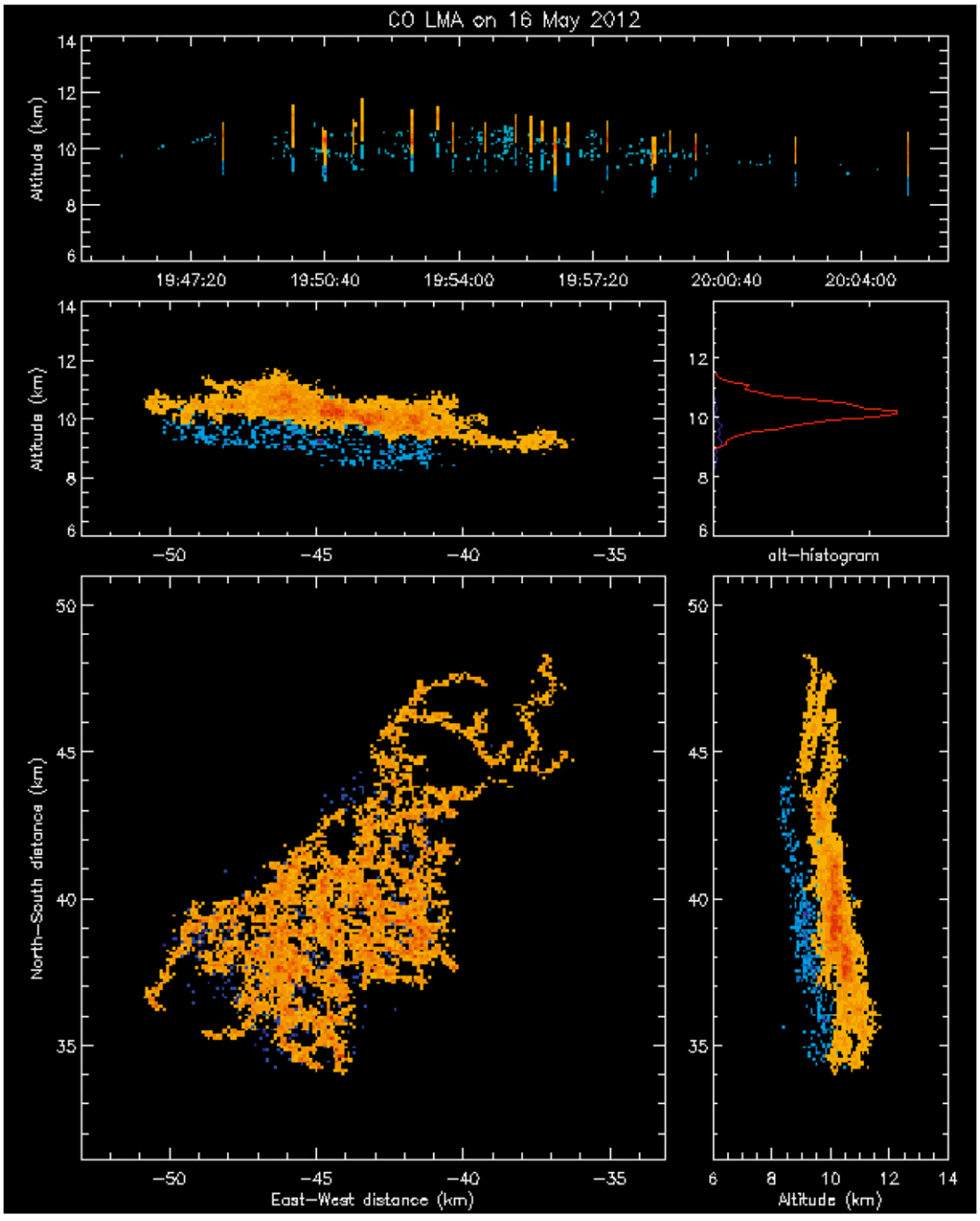

FIG. 3. As in Fig. 1, but for relative density of COLMA sources for all lightning in the Hewlett Gulch plume on 16 May 2012, colored by inferred charge. The warmer colors (orange to red) indicate increasing density of COLMA sources associated with positive charge, while the colder colors (light to darker blue) indicate increasing density of COLMA sources associated with negative charge.

portion of the plume, prohibiting useful calculation of specific differential phase K_{DP}. This was consistent with the lack of significant positive differential phase shifts that are associated with the presence of rainfall (Ryzhkov and Zrnić 1996) or large dendrites (Kennedy and Rutledge 2011), or negative phase shifts that are associated with vertical alignment of ice crystals in strong electric fields (Carey and Rutledge 1998).

The upper-level reflectivity behavior in the plume (from the NMQ composites) and its relationship to lightning flash rate were examined in more detail for this case (Fig. 6a). Prior to 1930 UTC, there was a short-lived

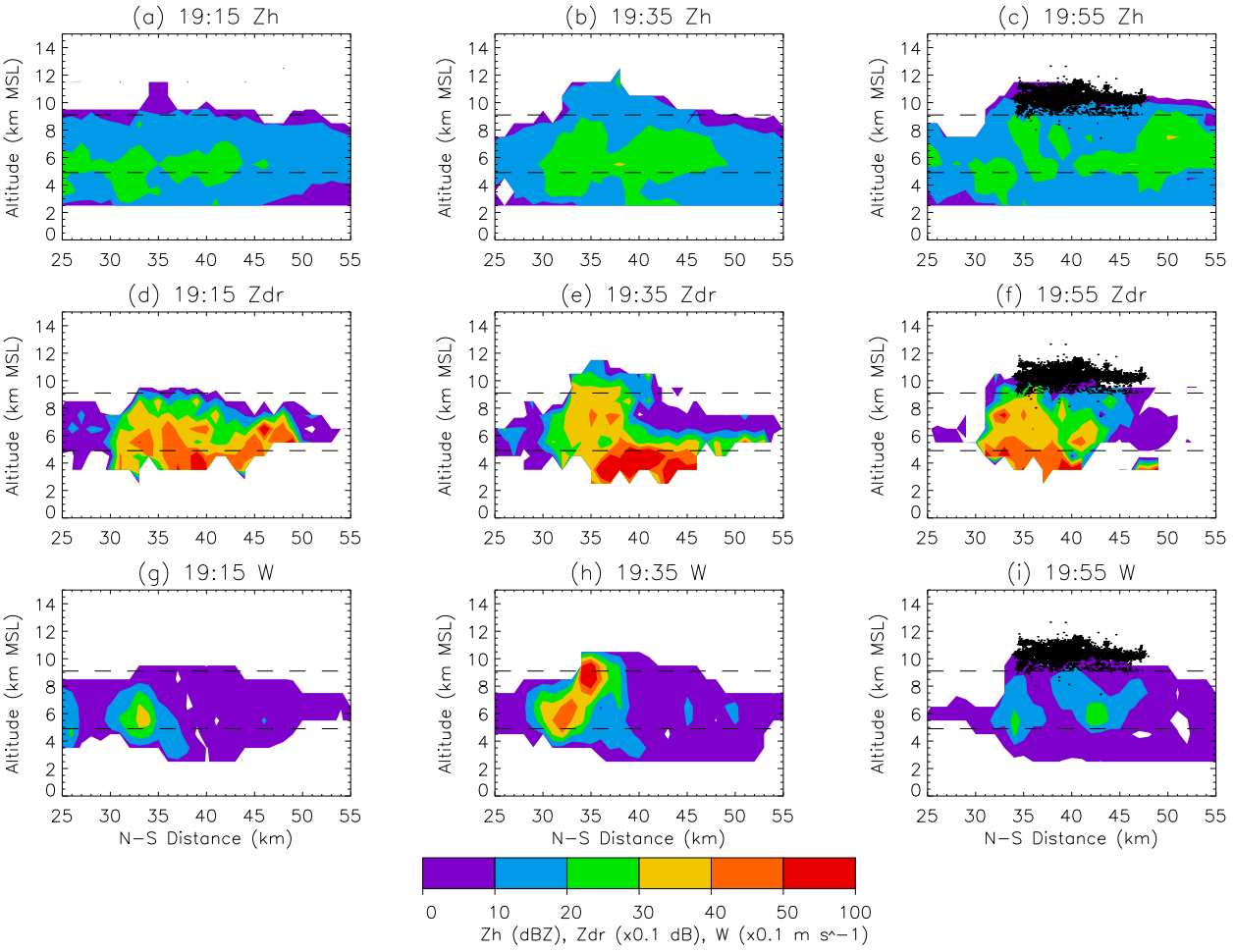

FIG. 4. *Y–Z* projections (between 250 km west of CSU–CHILL and 250 km east) of merged composite radar data for the Hewlett Gulch plume on 16 May 2012. (a)–(c) Merged maximum reflectivity Z_H (from CSU–CHILL, CSU–Pawnee, KCYS, and KFTG) at three separate UTC times. Also shown are COLMA-detected VHF sources (black dots) during each 5-min volume (no lightning occurred during the 1915 or 1935 UTC volumes), with the same projection, and dashed reference lines at the LCL and −40°C. (d)–(f) As in (a)–(c), but for differential reflectivity Z_{DR}, available only from CSU–CHILL. (g)–(i) As in (a)–(c), but for maximum vertical velocity W from the multi-Doppler synthesis. Note the different scales for Z_H, Z_{DR}, and W.

but initially large volume of 20-dBZ echo associated with the upper portion of a stratified layer of midlevel smoke and nonconvective cloud. Then, the 20-dBZ echo volume above 9 km MSL started increasing just before 1930 UTC, in response to the pyroconvective surge observed in Fig. 4. The plume lightning commenced during the 1945 UTC radar mosaic (maximum NMQ-estimated Z in the plume was 26.0 dBZ), shortly before the 20-dBZ echo volume achieved its maximum value (103 km^3 during the 1950 UTC mosaic), and did not last long after the volume began its permanent decline at 2000 UTC. Vertical mass flux (for regions where updrafts exceeded 2 $m\,s^{-1}$) from the multiple-Doppler retrieval also is shown in Fig. 6a. Mass flux peaked during the 1940–45 UTC synthesis volume, 3–8 min prior to the first lightning at 1948 UTC.

GOES shortwave IR (3.9 μm) imagery (Figs. 7a–c) shows that the lightning commenced after the pyrocumulus cloud had advected toward the northeast, revealing the hot spot ($T_B > 310$ K) at 1945 UTC that was previously covered by cloud at 1932 UTC. The lightning occurred approximately 10 km downwind of the thermal hot spot, in the northeastern portion of the radar-inferred plume. The plume itself also was downwind [east-northeast (ENE)] of the hot spot, indicating the effects the upper-level winds were having on the structure of the plume and the behavior of the lightning within it. Thermal hot spots are commonly used to identify fire locations at satellite wavelengths near 3.9 μm, and their temporal development can indicate fire intensification or growth (Weaver et al. 2004). The longwave IR (10.7 μm) channel (Figs. 7d–f) indicated the lightning occurred in a gradient region between cold cloud

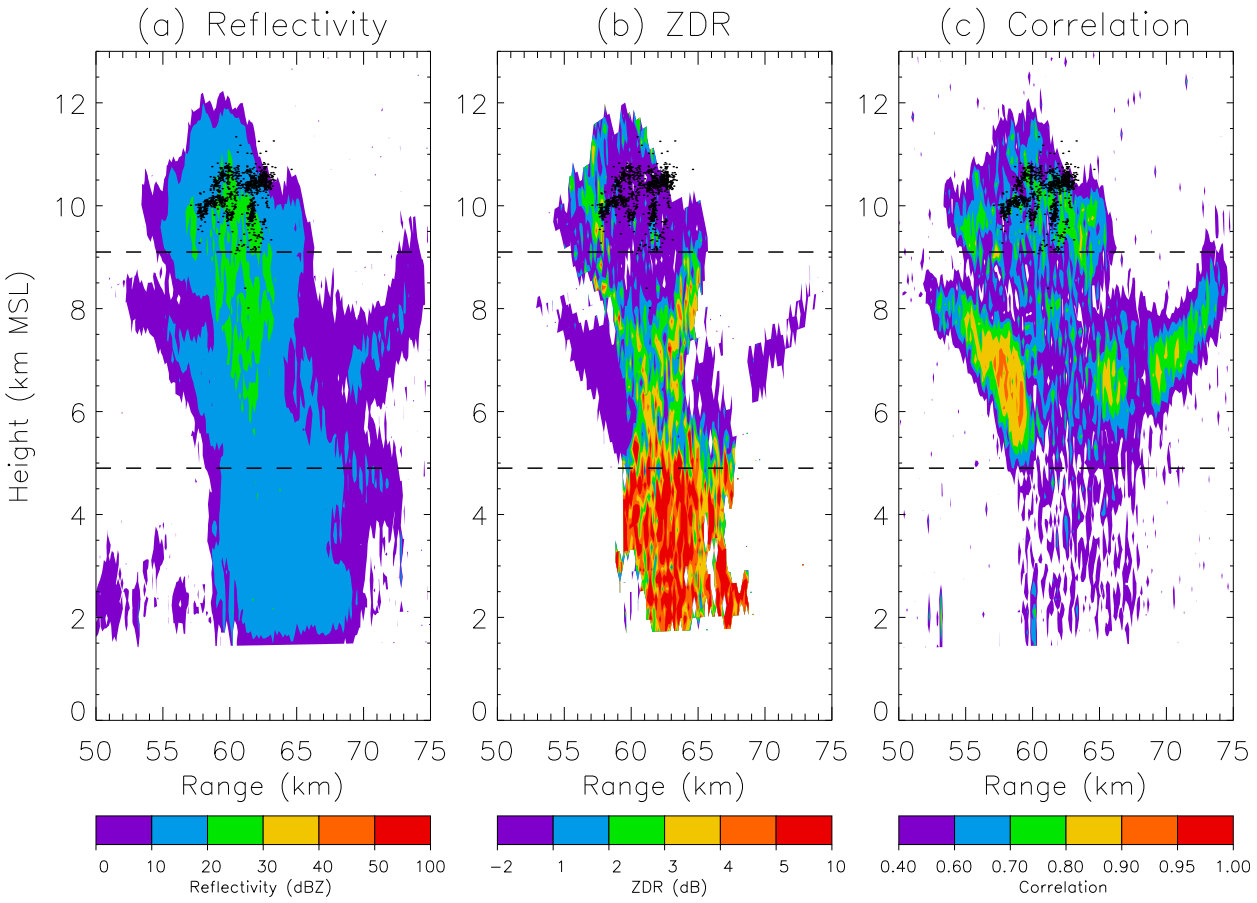

FIG. 5. Plots of CSU–CHILL (a) reflectivity, (b) differential reflectivity Z_{DR}, and (c) correlation coefficient from the RHI scan taken at 307° azimuth at 1949 UTC 16 May 2012. Sources from the lightning flash shown in Fig. 1 are also shown (black dots), projected onto the RHI. Also shown are dashed reference lines indicating the LCL and −40°C. This is the spatially and temporally closest RHI to this flash that is available.

($T_B \sim 220$ K or lower) associated with conventional, no-lightning-producing mountain convection ~10 km north of the fire and mostly clear skies over Fort Collins ~10 km southeast of the fire. These inferences are confirmed in the visible imagery from around the time of the plume electrification (Fig. 8), which shows the plume and associated pyroconvection advecting ENE of the fire, extending beyond the Colorado–Wyoming border.

In summary, the observations are consistent with the Hewlett Gulch plume electrifying and producing lightning after the fire intensified, increasing updrafts in the plume, which led to taller vertical development. However, the lightning preferentially favored regions containing inferred ice particles.

b. Other fires

1) HIGH PARK FIRE

The High Park fire, another fire near Fort Collins, was started by lightning that occurred during the local evening of 6 June 2012. However, the fire did not flare up and get reported until the morning of 9 June. The fire burned 87 824 acres (35 541 ha) along with 259 structures, and caused one fatality before it was fully contained on 1 July (Inciweb 2013b). The area burned was close to the location of the Hewlett Gulch fire, bordering the previous burn to its south and west. During the early days, the fire grew rapidly in size due to ample fuel and extremely dry weather. It was during the end of this first week of rapid growth, on the local afternoon of 13 June (a day when the fire burned approximately 3000 acres, or 1214 ha), that the smoke plume electrified and produced lightning. This was the only known instance of lightning-producing pyroconvection for this fire. The LCL from the 0000 UTC (14 June) sounding was close to 400 hPa (about −23°C or 7.5 km MSL). The freezing altitude was 4.9 km MSL, and the −40°C level was at 9.6 km MSL. Winds near 10 km MSL were from the WNW at ~15 m s^{-1}.

The plume above this fire was not scanned by the CSU radar assets during the lightning day. On days when

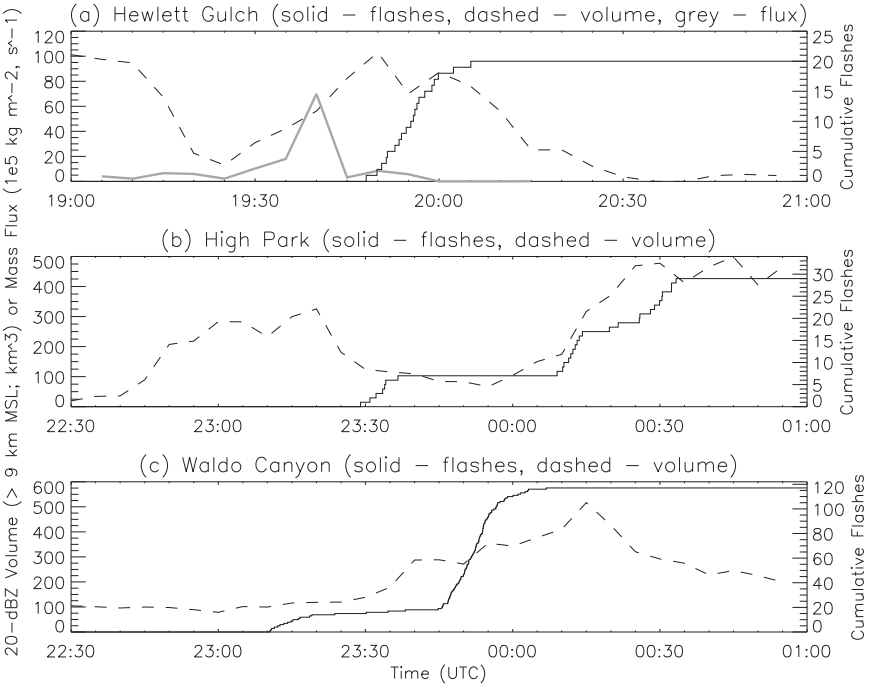

FIG. 6. Time series of 20-dBZ echo volume above 9 km MSL (dashed) and cumulative COLMA flash rates (solid; >10 sources per flash required) for the (a) Hewlett Gulch, (b) High Park, and (c) Waldo Canyon plumes during their lightning-producing time periods. Radar data are from the NMQ composites, and only include data within 0.15° latitude or longitude of the center of the plume lightning, spatial criteria that encompass the full extent of COLMA-detected lightning in any of the plumes. Also shown in (a) is the upward mass flux (gray solid) where updrafts exceed 2 m s^{-1}, as determined by multiple Doppler syntheses within the plume.

nonlightning-producing plumes above the High Park fire occurred and were visible by CSU radars (this commonly happened at least once every 2–3 days during the fire, because of active DC3 operations), they did not extend to the high altitudes observed on 13 June 2012. On these days, well-developed plumes reached ~6–8 km MSL maximum (an example from 22 June 2012 is shown in Fig. 9), and did not appear to contain ice-cloud caps based on the polarimetric data (i.e., Z_{DR} was not ~0 dB with $\rho_{HV} > 0.6$ like in the lightning-producing Hewlett plume). Indeed, despite reflectivities as large or larger than on the day the Hewlett Gulch plume produced lightning, the High Park example shown in Fig. 9 indicated very large Z_{DR} (>5 dB) in nearly every location within the plume, and ρ_{HV} did not reach the larger values seen aloft within the lightning-producing Hewlett Gulch plume. In addition, very little of the plume extended above the LCL, let alone the −40°C altitude. Other variables such as LDR and differential phase behaved similarly to the Hewlett Gulch plume.

National Weather Service (NWS) Doppler radars captured the evolution of the High Park plume on its lightning day, and the lightning was detected by the COLMA. Figure 10 shows the evolution of plume reflectivity (from the NMQ composites) and lightning above High Park fire (Figs. 10a–c). The electrification in the High Park plume behaved similarly to Hewlett Gulch, in that the development of modest reflectivities (10–25 dBZ) at high altitudes (10 km MSL/−43°C, or above) occurred prior to the lightning.

The High Park lightning mainly consisted of small ICs with limited vertical extent (1–2 km depth, similar to the Hewlett lightning). The High Park plume first produced a flash at 2328 UTC, and then produced 6 more over an 8-min period ending after 2336 UTC (0.9 min^{-1} flash rate; Fig. 6b). After a half-hour lull, lightning restarted at 0009 UTC and the plume produced 22 more flashes until 0033 UTC (0.9 min^{-1} flash rate). Note that these flash rates include only flashes that contained >10 LMA sources, and do not include the substantial precursor activity (1–2 sources apiece), which was similar in behavior to Hewlett Gulch. All of the lightning occurred in four distinct locations confined within a roughly 20 km × 20 km horizontal box downwind of the fire. Similar to Hewlett Gulch, increases in high-altitude 20-dBZ echo volumes led the initial lightning occurrence within the

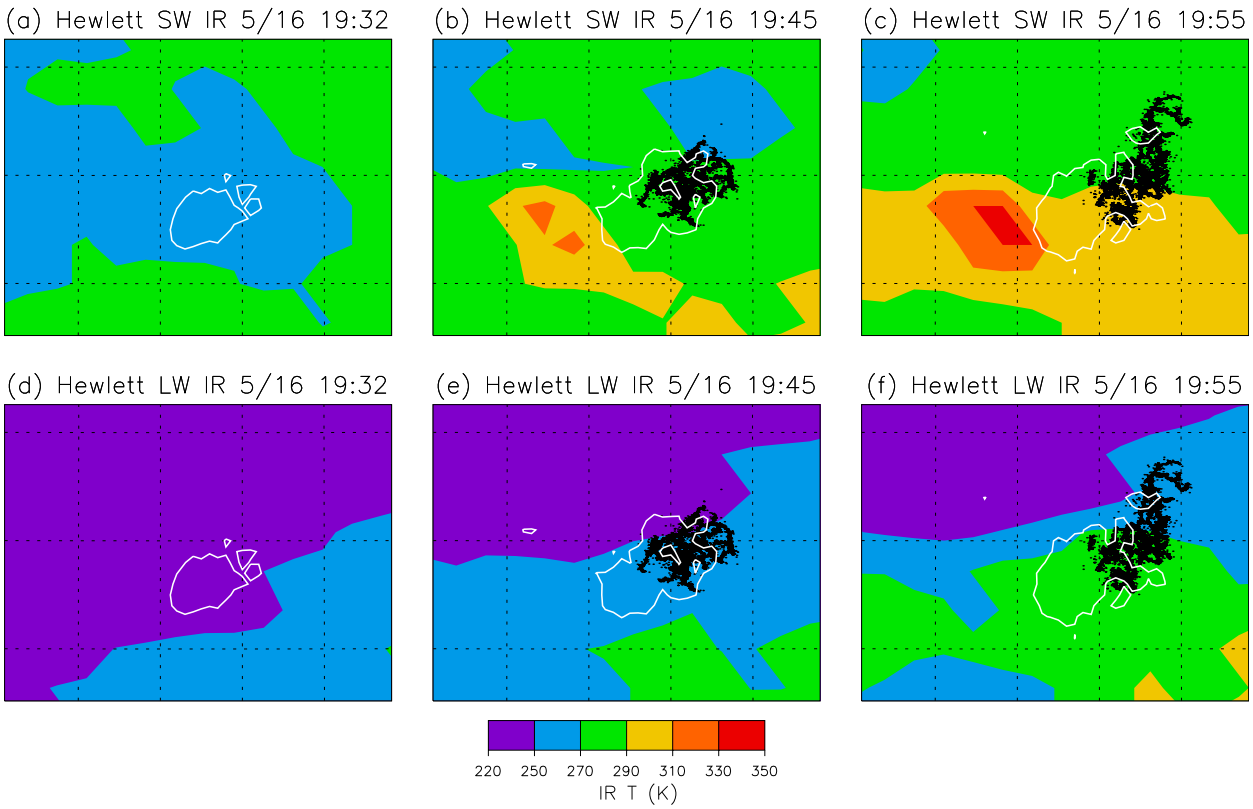

FIG. 7. GOES (a)–(c) shortwave and (d)–(f) longwave IR data at three different UTC times on 16 May 2012. Also shown in each plot are the COLMA-detected lightning sources (black dots), for 10 min after each listed time. The horizontal domain encompasses the Hewlett Gulch fire and immediate plume, and the dotted grid lines are spaced 0.1° in latitude and longitude. The 15-dBZ contour for NMQ composite reflectivities above 9 km MSL is shown in white.

plume, although the first lightning did not start until after this echo began declining (Fig. 6b). During the later lightning period, however, the flash counts and high-altitude echo volumes corresponded fairly well to one another, and the lightning ceased after 0030 UTC when the echo volumes plateaued.

The IC flashes tended to be smaller in size than the Hewlett Gulch ones (~1–2 km characteristic spatial dimension), with the exception of one flash (at 0028 UTC) that covered a much greater depth, roughly 6–11 km MSL (from −12° to −52°C; Fig. 10c). The greater depth was likely caused by a single downward-propagating negative leader. Overall, it was difficult to distinguish charge layers in the High Park case, as the small flashes did not exhibit the typical bilevel behavior observed in classic ICs (Rison et al. 1999). Assuming that negative leaders were mostly observed by the LMA, however, the data were consistent with positive charge just above 10 km MSL (−43°C), similar to Hewlett Gulch. The one exception was the single deep flash, which appeared to indicate positive charge also residing near midlevels, though this may have been short lived given the lack of repeat flashes in this layer.

The warm 3.9-μm brightness temperatures associated with the High Park fire hot spot can be seen in the western portion of Fig. 11a. Like the Hewlett Gulch case, the plume produced lightning after it had advected downwind to the east of the fire (Figs. 11b,c). Evidently, the stronger winds aloft assisted the greater physical displacement between the electrified plume and the fire itself, compared to Hewlett Gulch. The entire lightning-producing region contained cold longwave brightness temperatures (<270 K; Figs. 11d–f). Loops of visible imagery (not shown) indicated a large population of afternoon convective clouds over the northern Colorado foothills and mountains, along with a rapidly growing smoke plume.

2) WALDO CANYON FIRE

The Waldo Canyon fire started on 23 June 2012 west of Colorado Springs, Colorado. By the time it was contained on 10 July it had burned 18 247 acres (7384 ha), destroyed 346 structures, and caused two fatalities (Inciweb 2013c). The fire was human caused. On the afternoon of 26 June, the fire was whipped up by the

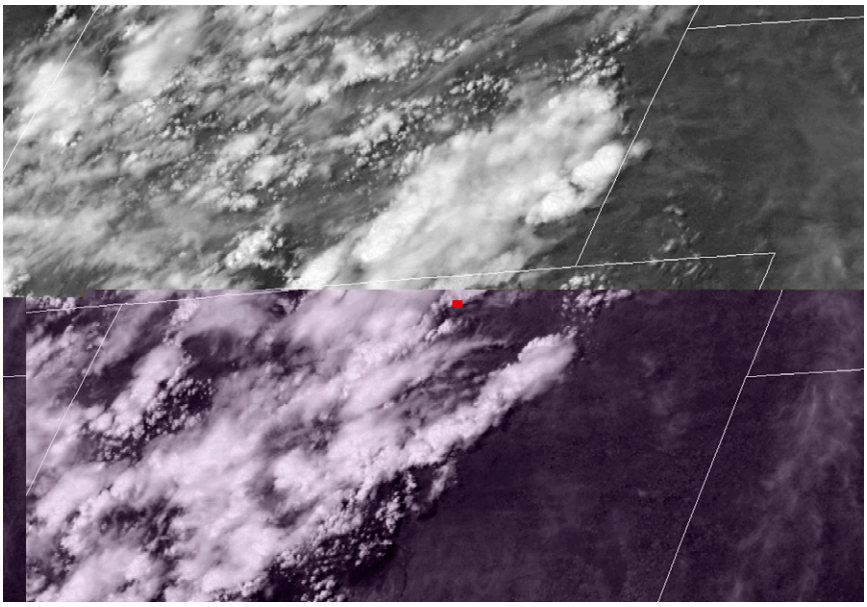

FIG. 8. *GOES-13* visible image at 1955 UTC 16 May 2012, with all corresponding 3.9-μm pixels having brightness temperatures exceeding 57°C colored black. The Hewlett fire hotspot shows up in the center of the image as two red pixels in north-central Colorado. The cloud extending to the northeast from the hotspot is pyroconvection.

passage of a strong gust front around 2300 UTC (Johnson et al. 2013). This led to deep vertical development of the plume and subsequent lightning production. This was the only known instance of lightning-producing pyroconvection for this fire. During and after this time portions of the Mountain Shadows subdivision near Colorado Springs were consumed as the rapidly spreading fire, which burned over 11 000 acres on this day (4452 ha), forced the evacuation of thousands of residents of the Colorado Springs area (Inciweb 2013c). The LCL from the 0000 UTC (27 June) sounding was close to 400 hPa (about −17°C or 7.6 km MSL). The freezing altitude was 5.2 km MSL, and the −40°C level was at 10.6 km MSL, significantly higher than the prior fire cases. Winds near 10 km MSL were mainly from the WSW at $\sim$5 m s^{-1}.

The Waldo Canyon fire was out of range of the CSU radars, but NWS radars scanned the plume on its lightning day (Figs. 10d–f). Once again, the development of modest reflectivities (10–25 dBZ) at high altitudes (10 km MSL/−35°C, or above) occurred prior to the lightning. The Waldo Canyon plume was more electrically active than the two preceding cases, with a total of 117 flashes (not counting precursors) during the period 2310–0006 UTC (2.1 min^{-1} flash rate; Fig. 6c). Similar to High Park, the lightning mainly came in two bursts. One started after 2310 UTC while 20-dBZ echo volumes were only gradually increasing. The second major burst occurred after 2345 UTC, which was led by a more rapid increase in high-altitude echo starting at 2335 UTC. Lightning terminated shortly before the 20-dBZ echo reached its peak at 0015 UTC.

The lightning appeared similar in size to Hewlett Gulch, and revealed a similar charge structure, though the greater range reduced the LMA's location accuracy (Thomas et al. 2004). At 2255 UTC (Fig. 10d)–just prior to the occurrence of plume lightning–there was a more conventional thunderstorm (near 39.2°N) approximately 30 km north of the fire (near 38.9°N). Another thunderstorm cell formed near this same northern position about a half hour later. After the electrified plume in Fig. 10e drifted northeastward with the prevailing winds, one of the last discharges in this northern thunderstorm (at 0039 UTC, well after the Waldo Canyon plume ceased producing its own discharges; Fig. 6c) propagated southward into the plume (Fig. 10f). This suggested that charge layers produced by the two clouds (one fire created, the other more conventional) may have merged.

In the Waldo Canyon case (Figs. 12a–c), flashes were observed with a convective burst just east of the hot spot at 2311 UTC (consistent with the weak WSW flow aloft observed in the sounding), and with a separate burst to the northeast of the fire at 0030 UTC. However, the conventionally electrified convection to the north of the fire appeared to be associated with a region of colder shortwave and longwave (Figs. 12d–f) brightness temperatures.

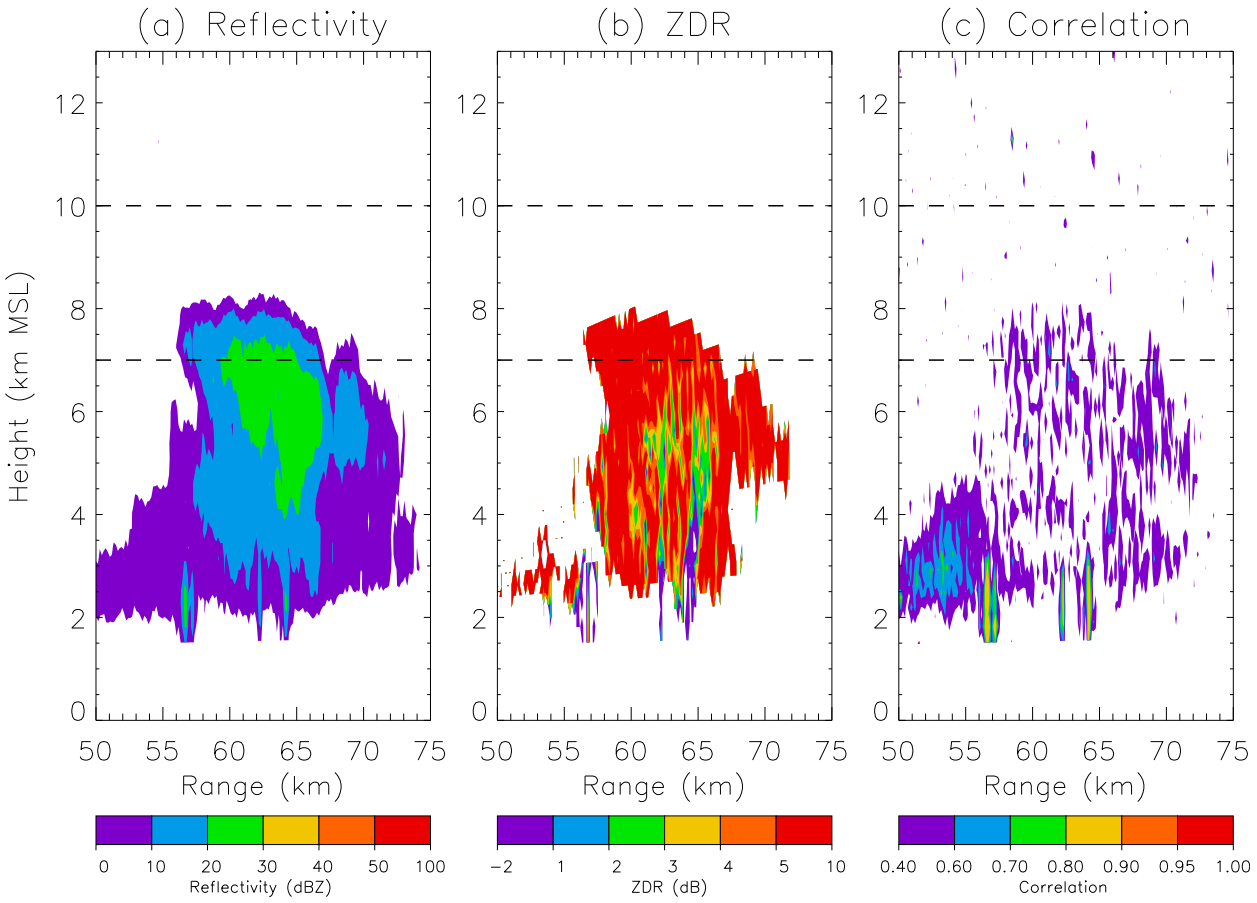

FIG. 9. As in Fig. 5, but for an RHI scan through the High Park plume at 301° azimuth, at 1956 UTC 22 Jun 2012. The plume did not produce lightning this day.

The aforementioned 0039 UTC flash originated from the northern thunderstorm (Figs. 12c,f) and traveled southward into a region of warmer brightness temperatures associated with the radar-inferred fire plume.

3) SUMMARY

In summary, the High Park and Waldo Canyon smoke plumes electrified and produced lightning under similar circumstances to the Hewlett Gulch plume. There was a rapidly growing fire (spectacularly so in the case of Waldo Canyon), plume development above 10 km MSL (from −35° to −43°C), lack of high reflectivities indicative of graupel, and (with some exceptions) the occurrence of infrequent, horizontally and vertically compact ICs at high altitudes. While the CSU–CHILL was not available to determine particle type in these latter two electrified plumes, the reflectivity structures were similar to Hewlett Gulch, except that the plumes were larger (Fig. 6), evidently due to fires with larger areas.

4. Discussion and conclusions

The evidence from these three cases suggests that pyrocumulus clouds atop smoke plumes electrified and produced small IC discharges under the following circumstances. A rapidly growing wildfire produces enhanced plume updrafts and vertical development. Meteorological instability allows the plume to extend above ~10 km MSL (i.e., air temperatures below −35° to −46°C, based on local soundings), where ice accumulates within the smoky plume. The lightning occurs within this region of inferred ice, and based on time series (Fig. 6) increased amounts of 20-dBZ echo or greater at high altitudes (inferred to include precipitation-sized and smaller ice particles, mixed with ash) need to occur prior to or in concert with the lightning. To the extent that it can be determined due to the lack of continuous polarimetric radar observations, high-altitude pyroconvection without significant amounts of radar-inferred ice did not produce any LMA-observed lightning over the three fires in this study.

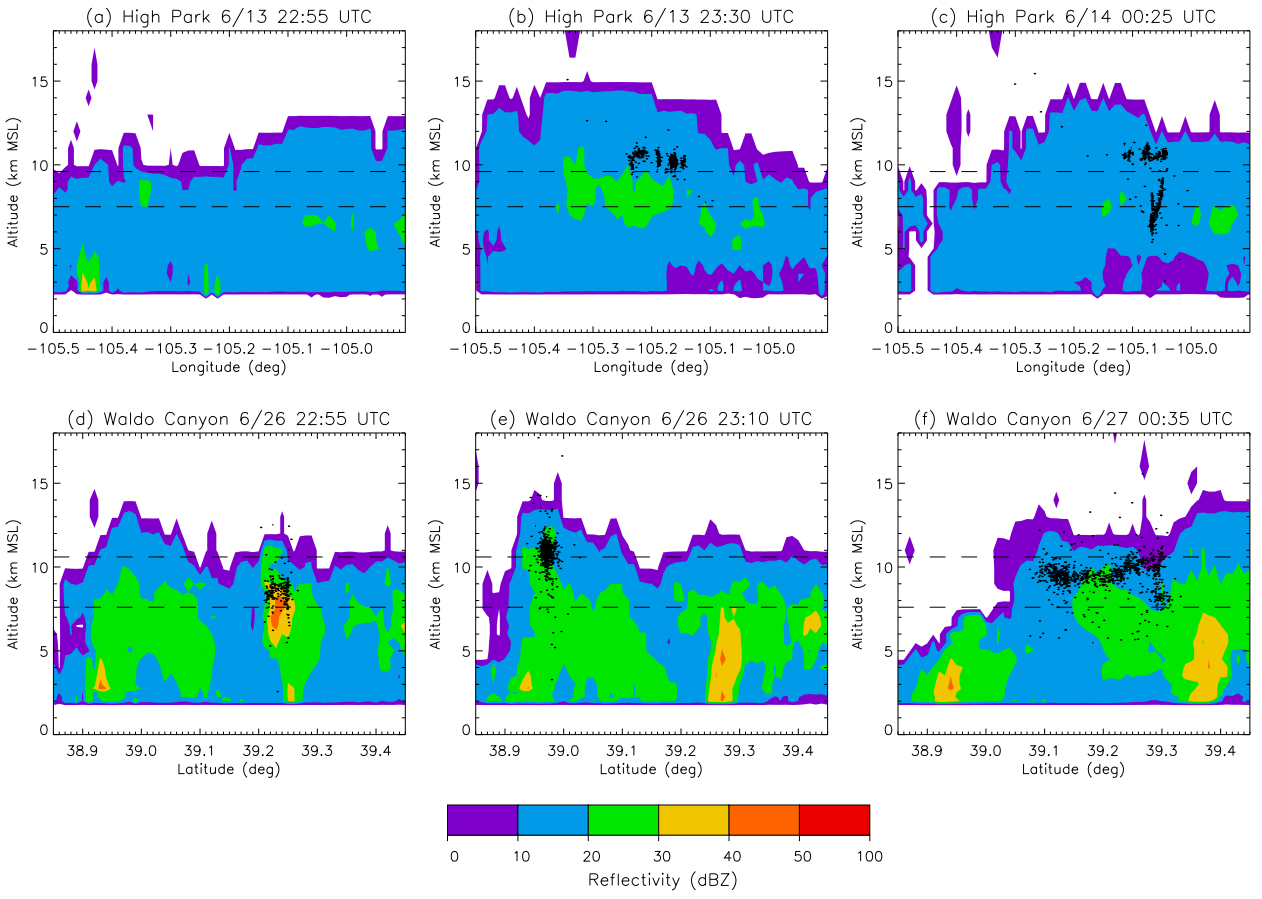

FIG. 10. (a)–(c) *X*–*Z* (longitude–height) projections (encompassing 40.5°–40.8°N latitude) of maximum NMQ reflectivity at three separate UTC times on 13–14 Jun 2012 in the High Park plume. Also shown are COLMA-detected VHF sources (black dots) during each 5-min volume, with the same projection, and dashed reference lines at the LCL and −40°C. (d)–(f) As in (a)–(c), but for *Y*–*Z* (latitude–height) projections (encompassing 105°–104.65°W longitude) in the Waldo Canyon plume.

The electrification mechanism thus is likely ice based, but the fact that lightning was observed at all is notable, given the weak reflectivity structure of the pyroclouds. For example, Lang and Rutledge (2011) determined that clouds with reflectivities <30 dB*Z* everywhere above the freezing altitude have only a ~10% chance to be concurrently producing lightning. This was likely due to the lack of significant amounts of high-density graupel in the mixed-phase region, which is an important driver of thunderstorm electrification (e.g., Takahashi 1978; Carey and Rutledge 1996; Wiens et al. 2005). Moreover, many of the weak cells that did produce lightning in the Lang and Rutledge (2011) dataset were later remnants of larger, stronger storms that did meet the 30-dB*Z* threshold at an earlier point in time. Such was not the case in the pyrocumulus clouds studied here.

Based on these observations, it is unclear whether a noninductive mechanism, which is postulated to occur during rebounding collisions between graupel and ice crystals in the presence of supercooled liquid water (Reynolds et al. 1957; Takahashi 1978; Jayaratne et al. 1983; Saunders et al. 1991), applies to these cases. The radar observations do not support the presence of significant amounts of high-density graupel. Reflectivities in lightning-producing plumes were capped near 25 dB*Z*, which is below the typical thresholds used to identify graupel in hydrometeor identification algorithms (e.g., Fig. 3 in Vivekanandan et al. 1999; Table 2 in Tessendorf et al. 2005).

In addition, the lightning occurred almost exclusively at high altitudes (~10 km MSL) where ambient temperatures were colder than −35°C (often much colder). Since liquid water droplets in clouds homogenously freeze when air temperature reaches −38°C or colder (Rosenfeld and Woodley 2000), it is uncertain that significant amounts of supercooled liquid water existed where the lightning was occurring. This is despite the fact that increased cloud water content is expected

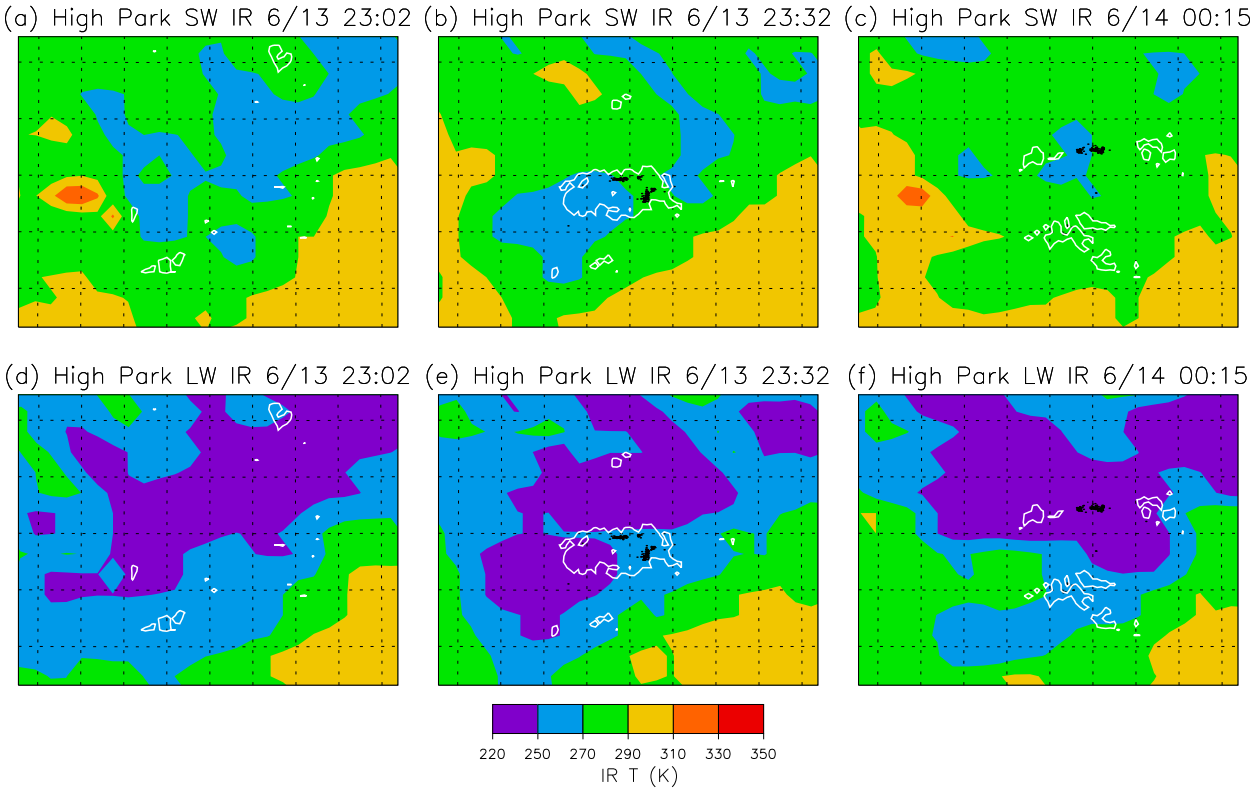

FIG. 11. GOES (a)–(c) shortwave and (d)–(f) longwave IR data at three different UTC times on 13–14 Jun 2012. Also shown in each plot are the COLMA-detected lightning sources (black dots), for 10 min after each listed time. The horizontal domain encompasses the High Park fire and immediate plume, and the dotted grid lines are spaced 0.1° in latitude and longitude. The 15-dBZ contour for NMQ composite reflectivities above 9 km MSL is shown in white.

under extremely high cloud condensation nuclei (CCN) concentration scenarios (e.g., ~5000 cm^{-3} and larger; Mansell and Ziegler 2013) that are partially representative of pyroclouds (Andreae et al. 2004). Of course, it may be possible that the heat of the fires increased temperatures within the plumes to be well above the sounding-derived air temperatures at any given altitude. This may have allowed some supercooled liquid water to exist at the high altitudes where the lightning was observed. However, the lack of a warm cloud layer in all of these cases may have prevented the development of large amounts of supercooled liquid water.

Alternatively, it is possible that the charging mainly occurred via noninductive processes at lower altitudes where supercooled liquid water could exist ($T > -38$°C; Rosenfeld and Woodley 2000), and was then "injected" to higher altitudes by a short-lived pulse of enhanced, fire-driven updrafts. There, at high altitudes where electric fields required for lightning initiation would be lower (due to lower air density), conditions would then be more favorable for lightning occurrence. The RHI scans of the Hewlett Gulch plume certainly indicated the presence of ice at midlevels (Fig. 5), as Z_{DR} values gradually decreased with increasing altitude, while ρ_{HV} increased—a transition from mostly ash particles near the fire to more abundant ice particles at high altitudes. This might explain the commonly observed lag periods between updrafts or high-level ice mass and the occurrence of lightning (Fig. 6), and would not necessarily rule out additional electrification occurring once the ice mass was lofted. In addition, portions of the region where lightning was occurring in the Waldo Canyon plume were slightly warmer than −38°C, based on the Denver sounding around that time.

It also is entirely possible, due to the weak nature of the electrification (mostly small, infrequent ICs), that an ice-based collision mechanism occurring in the absence of supercooled liquid water (e.g., Mitzeva et al. 2006; Ávila et al. 2011) may have been the principal driver of the observed lightning. Pyrocumulus clouds often feature ample amounts of ice that likely originated via homogeneous freezing of lofted cloud droplets (Lindsey and Fromm 2008). Moreover, electrification and lightning have been observed before in cold (i.e., $T < -38$°C) and therefore supercooled liquid water-deficient cloud regions (Rosenfeld and Woodley 2000) such as overshooting

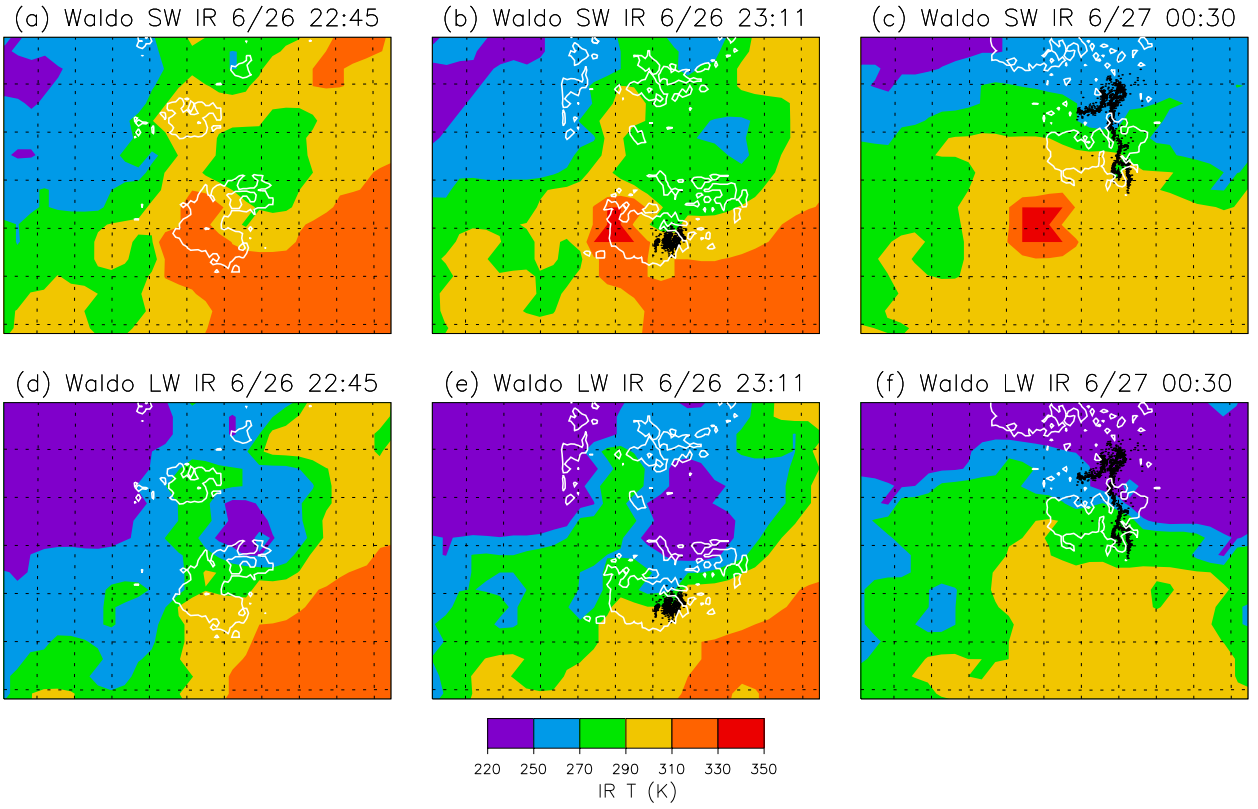

FIG. 12. GOES (a)–(c) shortwave and (d)–(f) longwave IR data at three different UTC times on 26–27 Jun 2012. Also shown in each plot are the COLMA-detected lightning sources (black dots), for 10 min after each listed time. The horizontal domain encompasses the Waldo Canyon fire, its immediate plume, and a conventional thunderstorm to the north. The dotted grid lines are spaced 0.1° in latitude and longitude. The 15-dBZ contour for NMQ composite reflectivities above 9 km MSL is shown in white.

cumulonimbus tops (Krehbiel et al. 2000; MacGorman et al. 2008; Meyer et al. 2013), as well as anvil clouds that are distant from parent convection (Dye and Willett 2007; Kuhlman et al. 2009). Thus, such a phenomenon occurring within high-altitude, cold, and therefore potentially supercooled liquid water-deficient (but ice rich) regions of pyrocumulus clouds is a reasonable supposition.

From their laboratory observations of ice particle charging at low temperatures in the absences of supercooled liquid water, Ávila et al. (2011) calculated a charging rate of $1\,\mathrm{C\,km^{-3}\,min^{-1}}$ (likely sufficient to produce lightning at high altitudes) provided a $3\,\mathrm{m^{-3}}$ number concentration of 4-mm diameter graupel particles. Assuming maximum ice density ($\sim$900 $\mathrm{kg\,m^{-3}}$), and using Smith (1984) to convert to equivalent radar reflectivity factor, yields $\sim$33 dBZ for this simulated microphysical situation, far in excess of what was observed in the 2012 Colorado pyrocumulus clouds. Thus, if there were graupel particles in them they likely were significantly less numerous, of lower density, and/or had smaller diameters than what was assumed in the example by Ávila et al. (2011), which implies a lower charging rate than $1\,\mathrm{C\,km^{-3}\,min^{-1}}$ by this mechanism. However, Ávila et al. (2011) did find negative charging of the graupel under this mechanism, which based on gravitational size sorting should lead to net positively charged small ice crystals above net negatively charged graupel or other large rimed particles, similar to the positive dipole observed in the 2012 pyroclouds. Weak charge separation may also occur during the freezing process (Mason and Maybank 1960; Ávila et al. 2003; Zilch et al. 2009), which is notable since lightning was observed at temperatures mainly below that required to trigger spontaneous freezing of supercooled liquid water.

Recently, Mansell and Zeigler (2013) performed simulations exploring the effects of CCN concentrations on the electrification of a simple thunderstorm. One of the notable results of the study was that, as CCN concentration increases, average graupel density tends to decrease at high altitudes, under extremely high CCN concentration scenarios. For example, Fig. 8d of Mansell and Ziegler (2013) shows an average graupel density of $\sim$400 $\mathrm{kg\,m^{-3}}$ at high CCN values ($\sim$5000 $\mathrm{cm^{-3}}$). Utilizing that density in the Ávila et al. (2011) example yields

an expected reflectivity of ~26 dBZ, much closer to the present observations. Though in situ observations do not exist to validate any of these microphysical assumptions, the main lesson is that a reduction in the mass density of graupel particles is expected at high CCN concentrations relevant to pyroclouds, and this could explain why the higher reflectivities (>30 dBZ) normally associated with graupel were not observed. The graupel may still be present, but simply have reduced particle mass density (Dolan and Rutledge 2009).

The most notable difference between the present observations and those in past studies of electrified pyroconvection (e.g., Latham 1991; Rosenfeld et al. 2007) is that no CG lightning flashes were produced from the 2012 Colorado cases. Indeed, the NLDN observed no lightning whatsoever. One reason for the lack of CG lightning may have been the relatively weak nature of the 2012 Colorado pyrocumulus clouds, especially compared to the significant Chisholm, Canada, firestorm (28 May 2001), which featured reflectivities in excess of 40 dBZ within it, suggesting significant amounts of high-density graupel (Rosenfeld et al. 2007). Unsurprisingly, high-resolution VHF networks like the COLMA provide a key advantage for studying pyrocumulus electrification because they can more easily detect small, weak IC discharges compared to VLF/LF networks like the NLDN, even at long range (~200 km) like the Waldo Canyon case. This also suggests that pyrocumulus lightning could occur much more frequently than implied from past studies that lacked access to detailed IC information.

There was little evidence of any inverted or anomalous electrical structures in these pyrocumulus clouds, in potential contrast to the observations of positive CG lightning in past studies of pyrocumulus (e.g., Latham 1991; Rosenfeld et al. 2007; Rudlosky and Fuelberg 2011). The lone exception to this statement was the single flash that descended to midlevels in the High Park plume, potentially indicating the short-lived presence of significant midlevel positive charge, but it is difficult to draw meaningful conclusions from a single event. Regardless, the vast bulk of the available evidence suggested a normal-polarity (positive over negative) dipole charge structure in the Colorado pyrocumulus, unlike the frequent observations of anomalous charge structures in other convection in this region (Lang and Rutledge 2011; Krehbiel et al. 2012; Lang et al. 2013).

Nevertheless, the observed mixtures of ash and ice in the lightning-producing cloud regions imply that ion-influenced electrification mechanisms such as those described by Vonnegut et al. (1995) or Jungwirth et al. (2005) could be operating in the present circumstances. The pyrocumulus clouds observed in Colorado during 2012 clearly would have included ample influence from ions attached to ash particles, which may have impacted ice-based charge-transfer processes. The present results also suggest an interesting point of comparison to electrification within similarly polluted cloud mixtures such as volcanic plumes, which likely electrify at least partially based on ice-based processes, particularly far from the eruption site (Williams and McNutt 2005; Thomas et al. 2007; Behnke et al. 2012).

Wildfire theory and models often predict plume height based on fire behavior and atmospheric stability parameters (e.g., Jenkins 2004; Coen et al. 2013). Given this present understanding, and given the unique characteristics of the lightning that occurred in smoke plumes observed in this study (isolated ICs with characteristic spatial dimensions of 1–5 km occurring in regions where $T \sim -40$°C or less), it is thus possible that lightning observations (of sufficient resolution and sensitivity) could be used to immediately identify wildfires undergoing rapid growth and manifesting deep pyroconvection. This may provide spatial and temporal advantages over satellite and radar data for identifying growing pyrocumulus clouds, and thus suggests a potential additional application for lightning data in assisting wildfire management. Also, since the lightning did not occur without the presence of significant radar-inferred (i.e., precipitation sized) ice, the presence (or lack thereof) of lightning in pyrocumulus has implications for the radiative characteristics and chemical composition of the upper troposphere. Future research is planned toward exploring how pyrocumulus lightning observations can be exploited to infer the characteristics of wildfires and pyroclouds in ways that may complement, substitute for, or even improve upon radar, satellite, and in situ observations.

Acknowledgments. Pat Kennedy, Bob Bowie, and Brody Fuchs of CSU assisted with the radar scanning for the Hewlett Gulch case. Paul Hein from CSU provided data and analysis support. Vaisala supplied the NLDN flash-level data analyzed in this study. The sounding data were obtained from the University of Wyoming web archive. Katherine Willingham provided the NMQ radar mosaic data on behalf of NOAA. The authors also thank the journal editor and reviewers for their assistance with publishing this study. This research was supported by the National Science Foundation (NSF) under Grant AGS-1010G6S7, as well as by the National Aeronautics and Space Administration (NASA) Marshall Space Flight Center's Fiscal Year 2013 Science Innovation Fund. NSF provided principal funding for DC3's Colorado ground-based facilities and operations. The views, opinions, and findings in this report are those of the authors, and

should not be construed as an official NASA, NOAA, or U.S. government position, policy, or decision.

REFERENCES

Andreae, M. O., D. Rosenfeld, P. Artaxo, A. A. Costa, G. P. Frank, K. M. Longo, and M. A. F. Silva-Dias, 2004: Smoking rain clouds over the Amazon. *Science,* **303,** 1337–1342.

Ávila, E. E., G. S. Longo, and R. E. Bürgesser, 2003: Mechanism for electric charge separation by ejection of charged particles from an ice particle growing by riming. *Atmos. Res.,* **69,** 99–108.

——, R. E. Bürgesser, N. E. Castellano, R. G. Pereyra, and C. P. R. Saunders, 2011: Charge separation in low-temperature ice cloud regions. *J. Geophys. Res.,* **116,** D14202, doi:10.1029/2010JD015475.

Barth, M. C., W. Brune, C. Cantrell, S. A. Rutledge, J. H. Crawford, F. Flocke, and H. Huntrieser, 2013: Overview of the deep convective clouds and chemistry experiment. Preprints, *Sixth Conf. on the Meteorological Applications of Lightning Data,* Austin, TX, Amer. Meteor. Soc., J7.1. [Available online at https://ams.confex.com/ams/93Annual/webprogram/Paper222132.html.]

Behnke, S. A., R. J. Thomas, P. R. Krehbiel, and S. R. McNutt, 2012: Spectacular lightning revealed in 2009 Mount Redoubt eruption. *Eos, Trans. Amer. Geophys. Union,* **93** (20), 193–194.

Bringi, V. N., R. Hoferer, D. A. Brunkow, R. Schwerdtfeger, V. Chandrasekar, S. A. Rutledge, J. George, and P. C. Kennedy, 2011: Design and performance characteristics of the new 8.5-m dual-offset Gregorian antenna for the CSU–CHILL radar. *J. Atmos. Oceanic Technol.,* **28,** 907–920.

Carey, L. D., and S. A. Rutledge, 1996: A multiparameter radar case study of the microphysical and kinematic evolution of a lightning producing storm. *Meteor. Atmos. Phys.,* **59,** 33–64.

——, and ——, 1998: Electrical and multiparameter radar observations of a severe hailstorm. *J. Geophys. Res.,* **103** (D12), 13 979–14 000.

Coen, J. L., M. Cameron, J. Michalakes, E. G. Patton, P. J. Riggan, and K. M. Yedinak, 2013: WRF-Fire: Coupled weather–wildland fire modeling with the Weather Research and Forecasting model. *J. Appl. Meteor. Climatol.,* **52,** 16–38.

Cummins, K. L., and M. J. Murphy, 2009: An overview of lightning locating systems: History, techniques, and data uses, with an in-depth look at the US NLDN. *IEEE Trans. Electromagn. Compat.,* **51** (3), 499–518.

Dolan, B. A., and S. A. Rutledge, 2007: An integrated display and analysis methodology for multivariable radar data. *J. Appl. Meteor. Climatol.,* **46,** 1196–1213.

——, and ——, 2009: A theory-based hydrometeor identification algorithm for X-band polarimetric radars. *J. Atmos. Oceanic Technol.,* **26,** 2071–2088.

Dye, J. E., and J. C. Willett, 2007: Observed enhancement of reflectivity and the electric field in long-lived Florida anvils. *Mon. Wea. Rev.,* **135,** 3362–3380.

Fromm, M., D. T. Lindsey, R. Servranckx, G. Yue, T. Trickl, R. Sica, P. Doucet, and S. Godin-Beekmann, 2010: The untold story of pyrocumulonimbus. *Bull. Amer. Meteor. Soc.,* **91,** 1193–1209.

Goodman, S. J., and Coauthors, 2005: The North Alabama lightning mapping array: Recent severe storm observations and future prospects. *Atmos. Res.,* **76** (1), 423–437.

Hufford, G. L., H. L. Kelley, W. Sparkman, and R. K. Moore, 1998: Use of real-time multisatellite and radar data to support forest fire management. *Wea. Forecasting,* **13,** 592–605.

Inciweb, cited 2013a: Hewlett fire. [Available online at http://www.inciweb.org/incident/2863/.]

——, cited 2013b: High Park fire. [Available online at http://www.inciweb.org/incident/2904/.]

——, cited 2013c: Waldo Canyon fire. [Available online at http://www.inciweb.org/incident/2929/.]

Jayaratne, E. R., C. P. R. Saunders, and J. Hallett, 1983: Laboratory studies of the charging of soft-hail during ice crystal interactions. *Quart. J. Roy. Meteor. Soc.,* **109,** 609–630.

Jenkins, M. A., 2004: Investigating the Haines Index using parcel model theory. *Int. J. Wildland Fire,* **13** (3), 297–309.

Johnson, R. H., R. S. Schumacher, and D. T. Lindsey, 2013: Weather impacts on the June 2012 Colorado Waldo Canyon Fire disaster. *Extended Abstracts, Impacts: Weather 2012,* Austin, TX, Amer. Meteor. Soc., 3.4. [Available online at https://ams.confex.com/ams/93Annual/webprogram/Paper224455.html.]

Jones, T. A., S. A. Christopher, and W. Petersen, 2009: Dual-polarization radar characteristics of an apartment fire. *J. Atmos. Oceanic Technol.,* **26,** 2257–2269.

Jungwirth, P., D. Rosenfeld, and V. Buch, 2005: A possible new molecular mechanism of thundercloud electrification. *Atmos. Res.,* **76,** 190–205.

Kennedy, P. C., and S. A. Rutledge, 2011: S-band dual-polarization radar observations of winter storms. *J. Appl. Meteor. Climatol.,* **50,** 844–858.

Khain, A. P., N. BenMoshe, and A. Pokrovsky, 2008: Factors determining the impact of aerosols on surface precipitation from clouds: An attempt at classification. *J. Atmos. Sci.,* **65,** 1721–1748.

Krehbiel, P. R., R. J. Thomas, W. Rison, T. Hamlin, J. Harlin, and M. Davis, 2000: GPS-based mapping system reveals lightning inside storms. *Eos, Trans. Amer. Geophys. Union,* **81** (3), 21–25.

——, W. Rison, R. Thomas, T. Hamlin, and J. Harlin, 2003: Lightning modes in thunderstorms. *2003 Fall Meeting,* San Francisco, CA, Amer. Geophys. Union, Abstract AE31A-06.

——, ——, and ——, 2012: Lightning mapping observations during DC3 in northern Colorado. *2012 Fall Meeting,* San Francisco, CA, Amer. Geophys. Union, Abstract AE12A-05.

Kuhlman, K. M., D. R. MacGorman, M. I. Biggerstaff, and P. R. Krehbiel, 2009: Lightning initiation in the anvils of two supercell storms. *Geophys. Res. Lett.,* **36,** L07802, doi:10.1029/2008GL036650.

Lang, T. J., and S. A. Rutledge, 2002: Relationships between convective storm kinematics, precipitation, and lightning. *Mon. Wea. Rev.,* **130,** 2492–2506.

——, and ——, 2006: Cloud-to-ground lightning downwind of the 2002 Hayman forest fire in Colorado. *Geophys. Res. Lett.,* **33,** L03804, doi:10.1029/2005GL024608.

——, and ——, 2008: Kinematic, microphysical, and electrical aspects of an asymmetric bow-echo mesoscale convective system observed during STEPS 2000. *J. Geophys. Res.,* **113,** D08213, doi:10.1029/2006JD007709.

——, and ——, 2011: A framework for the statistical analysis of large radar and lightning datasets: Results from STEPS 2000. *Mon. Wea. Rev.,* **139,** 2536–2551.

——, and Coauthors, 2013: Highlights of Colorado ground facility operations during DC3. Preprints, *Sixth Conf. on the Meteorological Applications of Lightning Data,* Austin, TX, Amer. Meteor. Soc., J7.2. [Available online at https://ams.confex.com/ams/93Annual/webprogram/Paper221524.html.]

Latham, D. J., 1991: Lightning flashes from a prescribed fire-induced cloud. *J. Geophys. Res.,* **96** (D9), 17 151–17 157.

——, 1999: Space charge generated by wind tunnel fires. *Atmos. Res.,* **51,** 267–278.

Lindsey, D. T., and M. Fromm, 2008: Evidence of the cloud lifetime effect from wildfire-induced thunderstorms. *Geophys. Res. Lett.,* **35,** L22809, doi:10.1029/2008GL035680.

Lyons, W. A., T. E. Nelson, E. R. Williams, J. A. Cramer, and T. R. Turner, 1998: Enhanced positive cloud-to-ground lightning in thunderstorms ingesting smoke from fires. *Science,* **282,** 77–80.

MacGorman, D. R., and Coauthors, 2008: TELEX: The Thunderstorm Electrification and Lightning Experiment. *Bull. Amer. Meteor. Soc.,* **89,** 997–1013.

Mansell, E. R., and C. L. Ziegler, 2013: Aerosol effects on simulated storm electrification and precipitation in a two-moment bulk microphysics model. *J. Atmos. Sci.,* **70,** 2032–2050.

Mason, B. J., and J. Maybank, 1960: The fragmentation and electrification of freezing water drops. *Quart. J. Roy. Meteor. Soc.,* **86,** 176–185.

Melnikov, V. M., D. S. Zrnić, R. M. Rabin, and P. Zhang, 2008: Radar polarimetric signatures of fire plumes in Oklahoma. *Geophys. Res. Lett.,* **35,** L14815, doi:10.1029/2008GL034311.

——, ——, and ——, 2009: Polarimetric radar properties of smoke plumes: A model. *J. Geophys. Res.,* **114,** D21204, doi:10.1029/2009JD012647.

Meyer, T. C., T. J. Lang, S. A. Rutledge, W. A. Lyons, S. A. Cummer, G. Lu, and D. T. Lindsey, 2013: Radar and lightning analyses of gigantic jet-producing storms. *J. Geophys. Res. Atmos.,* **118,** 2872–2888, doi:10.1002/jgrd.50302.

Miller, L. J., C. G. Mohr, and A. J. Weinheimer, 1986: The simple rectification to Cartesian space of folded radial velocities from Doppler radar sampling. *J. Atmos. Oceanic Technol.,* **3,** 162–174.

Mitzeva, R., C. Saunders, and B. Tsenova, 2006: Parameterisation of non-inductive charging in thunderstorm regions free of cloud droplets. *Atmos. Res.,* **82** (1), 102–111.

Mohr, C. G., and R. L. Vaughn, 1979: An economical approach for Cartesian interpolation and display of reflectivity factor data in three-dimensional space. *J. Appl. Meteor.,* **18,** 661–670.

——, L. J. Miller, R. L. Vaughn, and H. W. Frank, 1986: On the merger of mesoscale datasets into a common Cartesian format for efficient and systematic analysis. *J. Atmos. Oceanic Technol.,* **3,** 143–161.

Reynolds, S. E., M. Brook, and M. F. Gourley, 1957: Thunderstorm charge separation. *J. Meteor.,* **14,** 426–436.

Rison, W., R. J. Thomas, P. R. Krehbiel, T. Hamlin, and J. Harlin, 1999: A GPS-based three-dimensional lightning mapping system: Initial observations in central New Mexico. *Geophys. Res. Lett.,* **26,** 3573–3576.

Rosenfeld, D., 1999: TRMM observed first direct evidence of smoke from forest fires inhibiting rainfall. *Geophys. Res. Lett.,* **26,** 3105–3108.

——, and W. L. Woodley, 2000: Deep convective clouds with sustained supercooled liquid water down to −37.5°C. *Nature,* **405,** 440–442.

——, M. Fromm, J. Trentmann, G. Luderer, M. O. Andreae, and R. Servranckx, 2007: The Chisholm firestorm: Observed microstructure, precipitation and lightning activity of a pyrocumulonimbus. *Atmos. Chem. Phys.,* **7** (3), 645–659.

Rudlosky, S. D., and H. E. Fuelberg, 2011: Seasonal, regional, and storm-scale variability of cloud-to-ground lightning characteristics in Florida. *Mon. Wea. Rev.,* **139,** 1826–1843.

Ryzhkov, A., and D. Zrnić, 1996: Assessment of rainfall measurement that uses specific differential phase. *J. Appl. Meteor.,* **35,** 2080–2090.

Saunders, C. P. R., W. D. Keith, and R. P. Mitzeva, 1991: The effect of liquid water on thunderstorm charging. *J. Geophys. Res.,* **96** (D6), 11 007–11 017.

Smith, P. L., 1984: Equivalent radar reflectivity factors for snow and ice particles. *J. Climate Appl. Meteor.,* **23,** 1258–1260.

Takahashi, T., 1978: Riming electrification as a charge generation mechanism in thunderstorms. *J. Atmos. Sci.,* **35,** 1536–1548.

Tessendorf, S. A., L. J. Miller, K. C. Wiens, and S. A. Rutledge, 2005: The 29 June 2000 supercell observed during STEPS. Part I: Kinematics and microphysics. *J. Atmos. Sci.,* **62,** 4127–4150.

Thomas, R. J., P. R. Krehbiel, W. Rison, S. J. Hunyady, W. P. Winn, T. Hamlin, and J. Harlin, 2004: Accuracy of the Lightning Mapping Array. *J. Geophys. Res.,* **109,** D14207, doi:10.1029/2004JD004549.

——, and Coauthors, 2007: Electrical activity during the 2006 Mount St. Augustine volcanic eruptions. *Science,* **315** (5815), 1097.

Vivekanandan, J., S. M. Ellis, R. Oye, D. S. Zrnić, A. V. Ryzhkov, and J. Straka, 1999: Cloud microphysics retrieval using S-band dual-polarization radar measurements. *Bull. Amer. Meteor. Soc.,* **80,** 381–388.

Vonnegut, B., D. J. Latham, C. B. Moore, and S. J. Hunyady, 1995: An explanation for anomalous lightning from forest fire clouds. *J. Geophys. Res.,* **100** (D3), 5037–5050.

Weaver, J. F., D. Lindsey, D. Bikos, C. C. Schmidt, and E. Prins, 2004: Fire detection using GOES rapid scan imagery. *Wea. Forecasting,* **19,** 496–510.

Wiens, K. C., S. A. Rutledge, and S. A. Tessendorf, 2005: The 29 June 2000 supercell observed during STEPS. Part II: Lightning and charge structure. *J. Atmos. Sci.,* **62,** 4151–4177.

Williams, E. R., and S. R. McNutt, 2005: Total water contents in volcanic eruption clouds and implications for electrification and lightning. *Recent Progress in Lightning Physics,* C. Pontikis, Ed., Research Signpost Publishing, 81–93.

——, V. Mushtak, D. Rosenfeld, S. Goodman, and D. Boccippio, 2005: Thermodynamic conditions favorable to superlative thunderstorm updraft, mixed phase microphysics, and lightning flash rate. *Atmos. Res.,* **76,** 288–306.

Zhang, J., and Coauthors, 2011: National Mosaic and Multi-Sensor QPE (NMQ) System: Description, results, and future plans. *Bull. Amer. Meteor. Soc.,* **92,** 1321–1338.

Zilch, L. W., J. T. Maze, J. W. Smith, and M. F. Jarrold, 2009: Freezing, fragmentation, and charge separation in sonic sprayed water droplets. *Int. J. Mass Spectrom.,* **283,** 191–199.